A Reduced Model Retaining 1st-Order Vortex Corrections in the Averaged Dynamics of the Wind past Buildings

Samik Maiti[1,2], Aminallah Rabia[3*] , Amine Ammar[4] , Alessandro Biancalani[2] , Francisco Chinesta[5] , Yannick Hoarau[1] , Samir Yahiaoui[2]

[1] CNRS, ICUBE UMR 7357, University of Strasbourg, Strasbourg 67000, France
[2] Research Center, Léonard de Vinci Pôle Universitaire, Paris La Défense 92916, France
[3] Ecole Supérieure d'Ingénieurs Léonard de Vinci, Paris La Défense 92916, France
[4] LAMPA, Arts et Metiers Institute of Technology, Angers 49035, France
[5] PIMM Lab and ESI Chair, Arts et Metiers Institute of Technology, Paris 75013, France

Corresponding Author Email: aminallah.rabia@devinci.fr

ABSTRACT

The nonlinear dynamics of turbulence formed by the wind flowing near solid objects can be studied with a variety of different physical models, more or less numerically demanding. An application is the study of the formation of turbulence past buildings, with the goal of determining the no-fly zones for drones in smart cities. In this paper, we examine the Reynolds- averaged Navier-Stokes (RANS) model, which is popular in simulating the wind dynamics in small portions of a city. We compare the results with those of the Large-Eddy-Simulation (LES) model, more physically comprehensive, but more numerically demanding. The analysis of the vortex formation in the LES model helps estimating the 1st-order correction to add to the lighter RANS results. This constitutes the scheme of a reduced model, which takes the RANS model as a basis, on top of which an extra layer of the dimension of the main vortex, obtained with the LES simulation, is added. This reduce model can be used, for example, to estimate the no-fly zone with a higher level of accuracy with respect to the pure RANS, yet with a computational effort comparable to the pure RANS.

1. INTRODUCTION

Turbulence is ubiquitous in nature. It can be observed at a variety of different scales from the interstellar medium [1], down to weather events [2], and to the flow of a fluid at the human scale, like water in a river [3] or the wind in a city [4]. Turbulence is also present in non-neutral fluids like magnetic-confinement fusion plasmas, where it interacts with meso-scale zonal flows and global Alfvenic fluctuations, making the achievement of controlled nuclear fusion more challenging [5].

Turbulence is intrinsically nonlinear [6], and consequently the study of its dynamics requires comprehensive physical models. Direct numerical simulations (DNS) are the most comprehensive models, retaining all the physics of the Navier-Stokes (NS) equations, but in most cases their resolution leads to incredibly high computational times. In the large-eddy-simulation (LES) approach [7], while solving the Navier-Stokes equations, the flow associated with the large-scale motion only is solved, while the small-scales are filtered out. Although this approximation greatly accelerates the numerical speed, nevertheless, for many realistic cases, the LES model remains unpractical. A very popular approximation of the NS model is given by the Reynolds-averaged Navier-Stokes (RANS) equations [8]. The RANS equations are derived by averaging the Navier-Stokes equations. The computational

demand of RANS models becomes very affordable already for medium-size computers. On the other hand, RANS simulations lose the knowledge of the perturbed motion of the fluid, e.g. the size of vortices. An improvement of the LES model is the detached-eddy simulation (DES) model [9, 10]. The DES model divides the spatial domain of interest in a region near the solid bodies, where the RANS model is adopted, and the rest of the domain, where the LES model is used. Although there is some improvement in the simulation speed with respect to pure LES simulation, nevertheless the characteristic computational time of DES simulations remains of the same order of magnitude as for the LES. Moreover, physics far from the walls (which is the main interest of our paper) is still solved with the LES model. Therefore, in this paper, we label the DES model as a particular type of LES models.

Recently, the study of the turbulence dynamics due to the interaction of wind and buildings has been renewed by the growing projects of smart cities, where flying drones take an important role in building a net for transportation and data transmission [11, 12]. Calculating the trajectory of drones between the buildings requires the knowledge of those zones where the presence of turbulence makes flying risky: the no-fly zones [13]. The dynamics of the wind past buildings has been described in numerous papers in the past, like in the

previous studies [14-17]. Saeedi et al. [18] have performed DNS simulations for a flow over a wall mounted cylinder they find an excellent agreement with the experiment conducted by Bourgeois et al. [19] and Sattari et al. [20] in wind tunnel with an aspect ratio of 4 and Reynolds number of 12000. Due to the high computation cost, most of the studies we have found in literature use the popular RANS model, which can give a zeroth order estimation of the no-fly zones for drones in reasonable computational time.

In this paper, we consider a test case of a uniform wind flowing past a squared-cylinder building. Our study has the goal of looking for an intermediate model among the RANS and the LES.

Cotteleer et al. [21] demonstrate how combining LES and RANS can optimize computational efficiency while maintaining physical accuracy for urban wind flow simulations using the hybrid Flow-Based Stress-Blended Eddy Simulation (Fb-SBES) framework.

Longo et al.'s [22] study explores advanced turbulence models for flows around ground-mounted buildings, emphasizing the need for accurate predictions of vortex shedding and flow separation mechanisms in urban environments.

From this point of view, our task is similar to the task of Kotsiopoulou and Bouris [23]. In the study of Kotsiopoulou and Bouris [23], the model proposed by the authors to study the flow past a squared-cylinder building is the Very Large Eddy Simulation (VLES) model (already described by Speziale [24] for general classes of problems). Differently from the DES model, the VLES model treats differently the physics of the vortices far from the walls, with respect to the LES model. In particular, the VLES cuts out the dynamics of small perturbation, with a higher threshold with respect to the LES model. Although the DES model includes more physics with respect to the RANS, the computational time is much higher. Therefore, we seek an alternative solution whose speed is of the order of magnitude of the speed of the RANS.

We start by investigating the results of RANS and LES simulations. The no-fly zone is estimated by measuring the level of vorticity. We show that the no-fly zone estimated with LES simulation is slightly larger, and the difference is the characteristic size of the vortices visible in LES simulations. Consequently, we propose a reduced model based on RANS simulation, with the 1st order correction given by the estimated vortex size. Although this model is far from being a comprehensive predicting model for all regimes of winds in the city, we believe that this can be used as a first step for more refined models based on this novel principle.

The structure of the paper is the following. In section 2, the test case is described, by defining the geometry and the fluid regime. We choose a system with one building of squared-cylinder shape for this numerical experiment. In section 3, we discuss the physical models of RANS and LES simulations. In section 4, we start by describing the results of RANS simulations. With these simulations, we provide the basis for our reduced model, by designing the no-fly zone without second-order corrections. Secondly, we run a LES simulation to estimate the size of the main turbulence vortices. This piece of physics is included in our reduced model, by adding an extra layer of the size of the dominant vortices. Note that the approximate size of this vortices does not depend on the details of the geometry of the building. Therefore, a set of RANS simulations can be performed, with the same value of vortex size. From this point of view, this reduced model still has the same computational time of the RANS model, because the LES simulation must be performed only once. Finally, section 5 is dedicated to a summary of the results and discussion.

2. DESCRIPTION OF THE TEST CASE

2.1 Geometry and boundary conditions

The geometry used in this study consists of a square cylinder (see Figure 1) subjected to a turbulent air flow. This geometry has been used for several studies [14, 15, 18, 25]. The dimensions are based on those in reference [15], with a blockage ratio of 1.5%: ensuring negligible borders effects. The square cylinder has a height of h = 4d, where, d represents the cylinder's width. The overall size of the domain is equal to 29d × 18d × 15d. The square cylinder is located at a distance of 8d downstream from the inlet and 20d upstream from the outlet. Additionally, it is located 8.5d from the sides of the domain and 11d from the top surface.
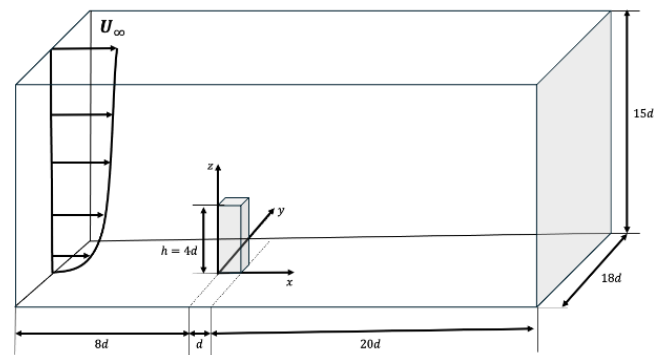

Figure 1. Virtual wind tunnel

The inlet chosen velocity profile is based on the study of Saeedi and Wang [25] where the authors reproduced numerically the experiments conducted in the studies of Bourgeois et al. [19] and Sattari et al. [20]. In fact, the wall mounted cylinder is exposed to a free-stream wind with an average velocity of $U_\infty = 15 m/s$ and a turbulence intensity of 0.8%.

The inlet velocity profile is modeled as in the study of Saeedi and Wang [25] using a power law as follows:

$$\begin{cases} \overline{u} = U_\infty \left(\dfrac{y}{0.15h} \right)^{0.16} & \text{for} \quad y < 0.15h \\ \overline{u} = U_\infty & \text{for} \quad y \geq 0.15h \end{cases}$$

The cylinder has a width of $d = 0.0127\,m$. Thus, the corresponding Reynolds number is:

$$\Re = \frac{U_\infty d}{\nu} = 12000$$

The square mounted cylinder is placed $2h$ downstream of the inlet boundary condition. Only a small portion of the square-cylinder is immersed in the thin boundary-layer thickness and 82% of the cylinder is above the boundary layer.

As the wind passes over the cylinder, von Karman vortices are alternatively produced. These vortex structures continuously evolve and interact within the wake region of the square cylinder.

2.2 Mesh

Our numerical calculation is performed using the open source CFD tool OpenFoam [26] version 9. Before solving the flow equation, a mesh has been performed using OpenFoam. It is consistent for such geometry to produce a structured mesh with hexahedral in shape cells. The mesh is produced into two steps using the tool Polymesh, first generating a basic mesh using blockMesh feature of the computational domain then a local refinement is performed at the building surfaces (near wall resolution) using "SnappyHexMesh" according to the expected value of Y+. Figure 2 shows the used mesh in a lateral view.
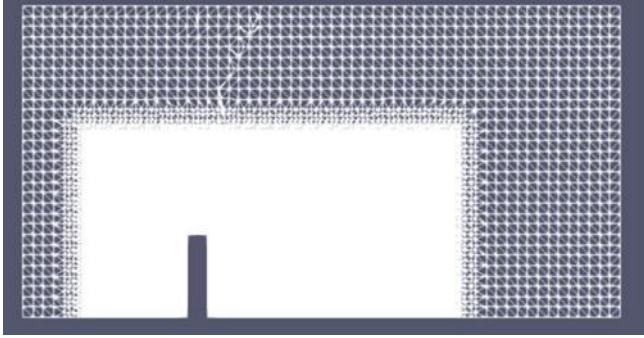

Figure 2. A lateral view of the generated Mesh

In order to obtain this mesh, the primary meshing in blockMesh is applied to the whole of computational domain 0.368 m × 0.228 m × 0.19 m. In secondary meshing with "snappyHexMesh" we choose to put "addlayer" feature on to create several inflation layers around the building geometry in order to control the first cell height of such a less value so that it will lie within the viscous sublayer and can accurately capture the physics of interaction between flow and the building surface. We did with creation of a refinement box of size 12d back of the building and 5d from all other surfaces of the building with 3rd grade refinement level in "snappyHexMesh" with the feature "refinementBox" for further refinement.
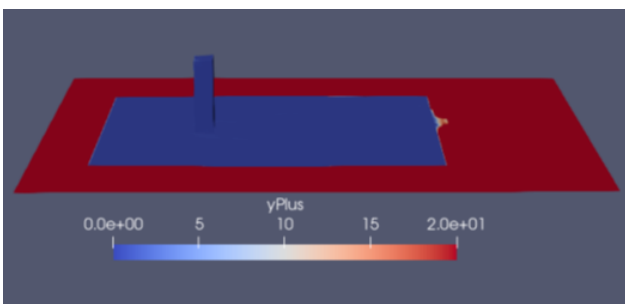

Figure 3. Yplus distribution at the ground and the square cylinder

Our intension is to keep Yplus value near 1 or as small as possible in the square cylinder vicinity (Figure 3). This makes us to go with feature of "add layer" in snappyHexMesh to add several inflations layers and adding inflation layer cause to mesh to gain non-orthogonality. Setting carefully the control parameter with "meshQualityControls" feature in snappyHexMesh, we can regulate the non-orthogonality within the permissible limit or safe level. This yields about 8 million hexahedra elements. The maximum aspect ratio of the mesh is 18.09. Regarding mesh non-orthogonality, the maximum value observed is 63.519, with an average of 3.505. Finally, the maximum skewness value is 1.34298. These statistics shows that all the mesh parameters are verified.

3. PHYSICAL MODELS

For this study we use Openfoam solver which solves numerically the incompressible Navier-Stokes (NS) equations (Eqs. (1) and (2)).

$$\frac{\partial u_i}{\partial x_i} = 0 \tag{1}$$

$$\rho \left[\frac{\partial u_i}{\partial t} + u_j \frac{\partial u_i}{\partial x_j} \right] = -\frac{\partial p}{\partial x_i} + \frac{\partial}{\partial x_j} \left[\mu \left(\frac{\partial u_i}{\partial x_j} + \frac{\partial u_j}{\partial x_i} \right) \right] \tag{2}$$

with u_i and x_i begin respectively the instantaneous velocity and position, p the instantaneous pressure, ρ the density, and µ the dynamic viscosity.

However, the direct numerical resolution of this system for our problem is too numerically expensive for present computers. Therefore, approximated models such as RANS and LES should be derived from the NS model.

On one side, the Reynolds-averaged Navier-Stokes (RANS) equations are derived by averaging the NS equations in time (see for example the study of Blocken et al. [8]). In RANS equations, only the mean part of the flow and fluctuation are retained. The RANS equations are obtained by decomposing the solution variables from the instantaneous NS equations into a time-average and a fluctuating component. For an instantaneous variable this means:

$$\phi = \bar{\phi} + \phi' \tag{3}$$

where, $\bar{\phi}$ is the mean and ϕ' the fluctuating component of the variable. Replacing the instantaneous variables in Eqs. (1) and (2) for an incompressible flow by the sum of the mean and the fluctuation components and taking an ensemble-average or time-average yields the RANS equations:

$$\frac{\partial \bar{u}_i}{\partial x_i} = 0 \tag{4}$$

$$\frac{\partial \bar{u}_i}{\partial t} + \bar{u}_j \frac{\partial \bar{u}_i}{\partial x_j} = -\frac{1}{\rho} \frac{\partial \bar{p}}{\partial x_i} + \frac{\partial}{\partial x_j} \left(2\nu \bar{S}_{ij} - \overline{u_i' u_j'} \right) \tag{5}$$

with the mean strain-rate tensor defined as:

$$\bar{S}_{ij} = \frac{1}{2} \left(\frac{\partial \bar{u}_i}{\partial x_j} + \frac{\partial \bar{u}_j}{\partial x_i} \right) \tag{6}$$

As for the closure model, we consider a first order, Spalart–Allmaras RANS model, which is a one-equation model, and the $k - \omega$ SST turbulence model which is a two-equation eddy-viscosity model [27].

RANS simulations are numerically very affordable. As an example, a typical RANS simulation for our test case can be performed in a personal computer. The drawback is that only the mean variables are given as output. So, RANS simulations are the best tool to provide a quick result which serves as 0-th order approximation of the realistic case.

On the other side, the large-eddy simulation (LES) model solves the NS equations after having applied a filter in space. The goal is to achieve a faster model compared to the direct numerical simulation (DNS) methods by means of solving only the large eddies with the NS model and using an approximation for the turbulence amplitude at smaller scales which does not require the resolution of the NS equations. The result is that the spatial mesh can be taken with a much lower number of points with respect to direct numerical simulation of the NS model, as the fine structures of turbulence are not solved in the mesh.

In the computational approach of LES, while solving the NS equations, the flow associated with are the large-scale motions solved, while the small-scale motions are filtered out, and are modeled. Additional unknowns arise from the filtering process, which must be addressed through modeling to achieve closure. A sub-filter turbulence model is used for this purpose.

A filtered or resolved variable denoted by an overbar is defined as:

$$\bar{f}(x) = \int_D \phi(x')G(x,x')dx' \qquad (7)$$

where, D is the entire domain and G is the filter function. The filter function determines the size and structure of the small scales.

where, $\bar{f}$ is the resolvable part and f' is the subgrid-scale part. By substituting this equation into the continuity and momentum conservation equations, and then applying filtering to the resulting expressions, the equations for the resolved field specifically, the filtered Navier-Stokes equations are obtained:

$$\frac{\partial \bar{u}_i}{\partial x_i} = 0 \qquad (8)$$

$$\frac{\partial \bar{u}_i}{\partial t} + \frac{\partial \bar{u}_i \bar{u}_j}{\partial x_j} = -\frac{1}{\rho}\frac{\partial \bar{p}}{\partial x_i} - \frac{\partial \tau_{ij}}{\partial x_j} + \nu\frac{\partial^2 \bar{u}_i}{\partial x_i \partial x_j} \qquad (9)$$

where, $\bar{u}_i$ and $\bar{p}$ are the resolvable velocity and resolvable pressure.

$\tau_{ij} = \overline{u_i u_j} - \overline{u_i}\,\overline{u_j}$ represents the subgrid-scale (SGS) stress term which must be modeled.

A particular type of turbulence models named detached-eddy simulation (DES), have been introduced by Spalart [9], Travin et al. [10] and Spalart [28] to increase the speed of simulations with respect to pure LES simulations. The idea of the DES model is to divide the spatial domain in a region far from the walls, where the LES model is used, and a region near the walls, where the RANS model is used. The simulation speed is increased because for DES simulations, the spatial grid is coarser than for pure LES simulations. From this point of view, the DES model is sometimes referred to as a hybrid RANS-LES models. In this paper, we adopt the DES model to have faster simulations with respect to the pure LES. On the other hand, as we are interested only in the physics far from the walls, we do not get a different description with the DES with respect to the LES, so we label the DES as a particular type of LES models. LES will be the way we will refer to these simulations in the following sections.

For our study a typical simulation takes 13 days using parallel computation with 96 processors.

## 4. REDUCED COST MODEL WITH VORTEX CORRECTIONS

In this section, we describe the zone of strong vorticity, generated by the interaction of the wind and the building. RANS simulations are computationally much less demanding but provide less details information on the turbulence structures. On the other hand, LES simulations while more computationally intensive, offer a richer representation of physics. Here, we compare the results of these two approaches and propose a procedure which can serves as reduced model, capable of achieving reasonable accuracy, without the high computational demand of LES simulations.
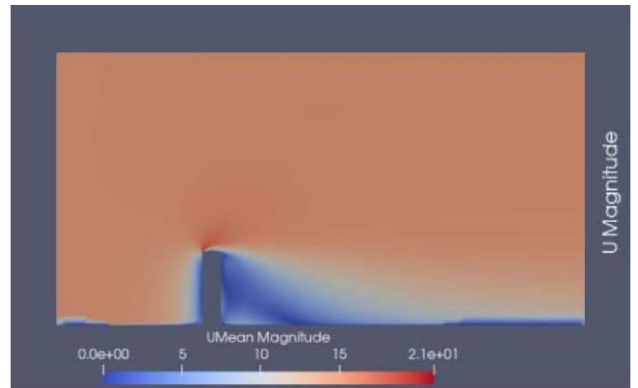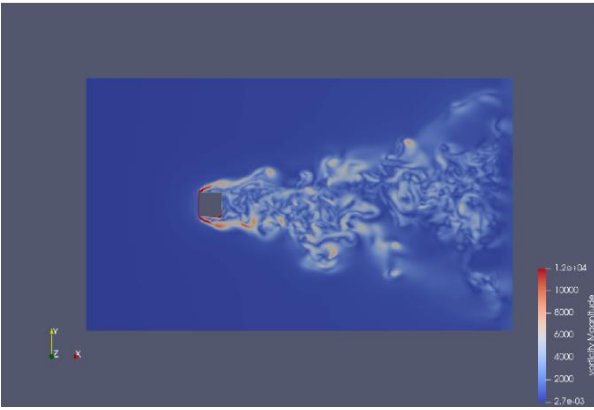
(a) Velocity [m/s] as a result of RANS simulations (vertical middle cutting plan)
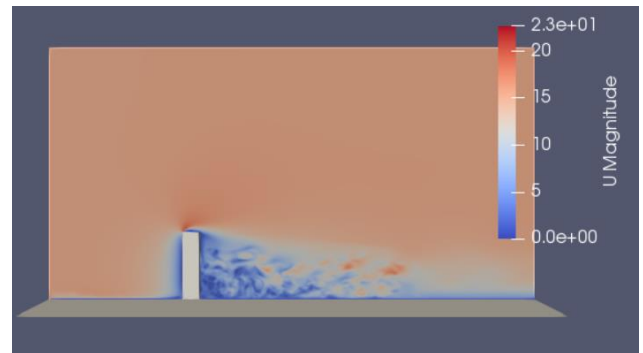
(b) Velocity [m/s] as a result of LES simulations (vertical middle cutting plan)
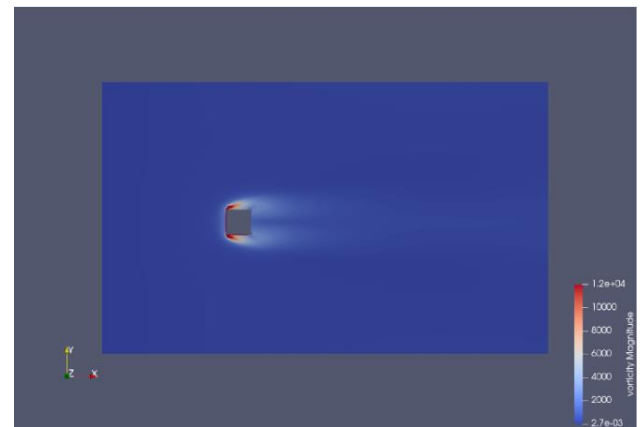
(c) Vorticity [s^{-1}] as a result of RANS simulations (cut at the half elevation)

(d) Vorticity [s^{-1}] as a result of LES simulations (cut at the half elevation)

Figure 4. Velocity and vorticity resulting from RANS simulations and LES simulations

Selected results from both turbulence models are presented in Figure 4 illustrating velocity and turbulence distribution in the middle vertical plan and in the horizontal plan at the elevation $z = h/2$. By comparing Figures 4(a) and 4(c) with Figures 4(b) and 4(d), we observe that the LES model provides more realistic details particularly in capturing the turbulence flow structures in the wake. This is due to the fundamental difference between the two methods for handling turbulence in the flow equations: RANS involves time averaged equations, whereas LES resolves larger turbulence scales. As a result, it is noticed that the region of high vorticity magnitude is significantly larger in the LES model than RANS model.
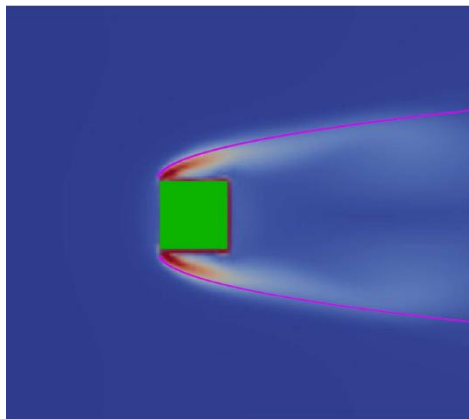
(a)
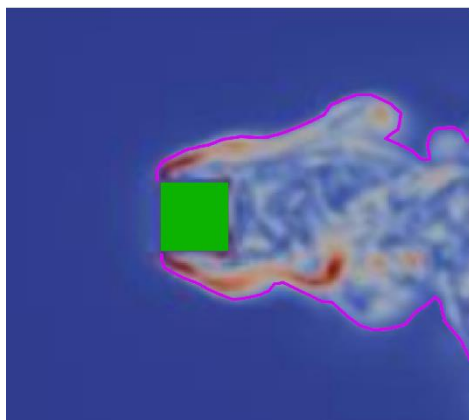
(b)

Figure 5. (a) No-fly zone in RANS; (b) No-fly zone in LES

To define the no-fly zone based on RANS simulations, we delimit the region with a non-negligible vorticity, shown in Figure 5(a). For LES simulations, the limit of no-fly zone is depicted in Figure 5(b). While the RANS model averages out spatial perturbations, making it easier to approximate the no-fly zone with a polynomial curve, the LES model reveals more complex dynamics. The LES no-fly zone contains vortices across a range of spatial scales, from small to large, which we denote as Δ.

It's important to note that defining no-fly zones accurately requires additional parameters and information beyond what is considered here. However, in this paper, we focus primarily on the role of turbulence intensity in shaping these zones.

To enhance the RANS-based no-fly zone, we propose a hybrid method. This method uses the RANS result as a baseline and adds higher-order correction based on the LES findings. Specifically, we note that the RANS approximation works well when the spatial perturbations are averaged out, but it omits the larger vortices. Therefore, we suggest enlarging the RANS-based no-fly zone by an additional layer equal to half the size of the largest LES vortices (Δ/2), as these large vortices could destabilize flying objects such as drones. This correction is shown in Figure 6 for our test case. The specific procedure is the following:

Step 1: Estimate the dominant vortex size with one LES simulation. For this simulation, one simulation with only one building is sufficient.

Step 2: Perform a set of RANS simulations with different buildings or entire parts of the city and draw the no-fly zone of the RANS simulations.

Step 3: Take the no-fly zones of the RANS simulations, and add an extra layer calculated from the result of step 1. This step will provide a larger no-fly zone, which is safer than that obtained in step 2.
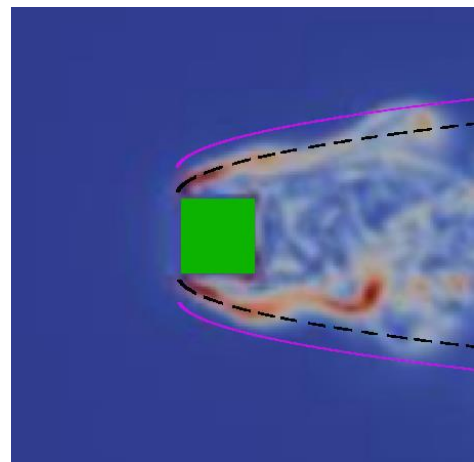

Figure 6. No-fly zone in LES simulations, described with the upgraded RANS estimation (pink lines)
Note: The original estimation given by the RANS simulations is also shown as a black dashed line, for comparison

Note that the method of the LES simulation in step 1 is very numerically demanding, but the simulation has a reasonable computational time since we restrict it to one building. This LES simulation is performed once-for-all. The RANS simulations are much faster, and they provide the characteristic computational time of the reduced model proposed here. Note also that, in this paper, we provide the proof of principle of the procedure, with a test simulation. In the implementation given for production runs, we propose to make scans of LES simulation in the building size, and wind

velocities, in order to create a table of values of Δ in dependence on these quantities.

The flow patterns given in Figure 6 were obtained for the same air speed at the entry of the virtual wind tunnel. However, we expect a change for different flow speeds. Typically, flows over a bluff- body exhibit several complex mechanisms such as the formation of boundary layer and the flow separation producing the vortex shedding that need to be carefully investigated. These mechanisms require careful analysis, as the value of Δ depends on the flow conditions. We recommend investigating the variation of Δ in the vicinity of the square cylinder to determine the appropriate level of correction to apply to the RANS results.

A precise estimation of the layer size is beyond the scope of this paper. We provide a first approximation of the layer size $\Delta \simeq d$ with d being the cylinder width. This is also consistent with the results of the study of Bouris and Bergeles [29]. The investigation of the dependence of the layer size on the parameters of the problem will be the topic of a dedicated paper.

5. CONCLUSIONS

In this paper, we investigated the formation of turbulence due to the interaction of the wind with a building. Such a problem has multiple applications: from the architectural point of view to the prediction of interaction with transportation means, to the design of recreational spaces for pedestrians.

The study focused on numerical simulations adopting two key models: large-eddy-simulation (LES) and Reynolds-averaged Navier-Stokes (RANS). Both models are derived from Navier-Stokes (NS) equations, with different levels of approximations to manage the computational cost of simulating turbulent flows. While LES resolves large scale turbulence and provides detailed insights into vortex dynamics, it is computationally expensive. RANS by contrast, is faster consists in averaging the NS equation, thus keeping only the mean velocities, and losing track of the perturbations.

Our primary focus in this paper was to predict the turbulence level around buildings to identify safe flight zones for drones, which is crucial in the context of smart city design and development. Drones can play a role in such environments by performing tasks like real time monitoring of temperature, pollution levels and health needs. Ensuring safe operation requires the identification of the so-called no-fly zones, areas with high turbulence levels that could destabilize drone flight.

Given that modeling wind interactions across large urban areas using LES is computationally prohibitive, we developed a compromise approach that combines the strengths of both LES and RANS. A similar effort of LES simulation of large urban areas has also been recently done in the study of Giersch et al. [30]. Our reduced model enables large-scale RANS simulations while incorporating higher-order corrections to account for the larger vortices typically captured by LES. Specifically, we propose conducting LES on a single building to estimate the size of significant vortices in the turbulence spectrum. This information is then used to adjust the RANS-predicted no-fly zones by adding a layer with a size proportional to half the largest vortex diameter (Δ/2).

The practical implications of this work are significant. The proposed model provides a scalable solution for predicting no-fly zones in urban environments without the prohibitive computational demands of LES. This approach could assist urban planners and engineers in the safe integration of drone technologies into smart cities, enhancing safety while enabling innovative urban services.

While this work presents a promising approach, further research is required to enhance the precision and applicability of the model. Future studies could focus on exploring the influence of varying wind conditions on turbulence structures, refining the estimation of Δ and understanding its dependence on environmental factors. Expanding the model to more complex urban environments with multiple buildings would also allow for better predictions of wind interactions in intricate city layouts. Additionally, research into real-time adaptive simulations could enable drones to dynamically adjust their flight paths based on live turbulence data. Investigating the aerodynamic factors of drones themselves may provide further insight, as their interactions with turbulent structures could necessitate additional corrections to the predicted no-fly zones. By addressing these areas, the safety and reliability of drone operations in urban settings can be further improved, advancing the integration of drone technologies into smart-city infrastructures.

REFERENCES

[1] Cerri, S.S., Passot, T., Laveder, D., Sulem, P.L., Kunz, M.W. (2022). Turbulent regimes in collisions of 3D Alfvén-wave packets. The Astrophysical Journal, 939(1): 36. https://doi.org/10.3847/1538-4357/ac93fe

[2] Zhao, Z., Gao, R., Zhang, J.A., Zhu, Y., Liu, C., Chan, P.W., Wan, Q. (2022). Observations of boundary layer wind and turbulence of a landfalling tropical cyclone. Scientific Reports, 12(1): 11056. https://doi.org/10.1038/s41598-022-14929-w

[3] Franca, M.J., Brocchini, M. (2015). Turbulence in rivers. In Rivers–Physical, Fluvial and Environmental Processes, pp. 51-78. https://doi.org/10.1007/978-3-319-17719-9_2

[4] Letzel, M.O., Helmke, C., Ng, E., An, X., Lai, A., Raasch, S. (2012). LES case study on pedestrian level ventilation in two neighbourhoods in Hong Kong. Meteorologische Zeitschrift, 21(6): 575-589. https://doi.org/10.1127/0941-2948/2012/0356

[5] Biancalani, A., Bottino, A., Di Siena, A., et al. (2021). Gyrokinetic investigation of Alfvén instabilities in the presence of turbulence. Plasma Physics and Controlled Fusion, 63(6): 065009. https://doi.org/10.1088/1361-6587/abf256

[6] Kolmogorov, A.N. (1991). The local structure of turbulence in incompressible viscous fluid for very large Reynolds numbers. Proceedings of the Royal Society of London, Series A: Mathematical and Physical Sciences, 434(1890): 9-13. https://doi.org/10.1098/rspa.1991.0075

[7] Smagorinsky, J. (1963). General circulation experiments with the primitive equations: I. The basic experiment. Monthly Weather Review, 91(3): 99-164.

https://doi.org/10.1175/1520-0493(1963)091%3C0099:GCEWTP%3E2.3.CO;2

[8] Blocken, B., Stathopoulos, T., Van Beeck, J.P.A.J. (2016). Pedestrian-level wind conditions around buildings: Review of wind-tunnel and CFD techniques and their accuracy for wind comfort assessment. Building and Environment, 100: 50-81. https://doi.org/10.1016/j.buildenv.2016.02.004

[9] Spalart, P.R. (2000). Strategies for turbulence modelling and simulations. International Journal of Heat and Fluid Flow, 21(3): 252-263. https://doi.org/10.1016/S0142-727X(00)00007-2

[10] Travin, A., Shur, M., Strelets, M., Spalart, P. (2000). Detached-eddy simulations past a circular cylinder. Flow, Turbulence and Combustion, 63(1): 293-313. https://doi.org/10.1023/A:1009901401183

[11] Stenvot, L. (2021). Leading CNRS project on hybrid AI launched in Singapore. https://news.cnrs.fr/articles/leading-cnrs-project-on-hybrid-ai-launched-in-singapore.

[12] Gao, M., Hugenholtz, C.H., Fox, T.A., Kucharczyk, M., Barchyn, T.E., Nesbit, P.R. (2021). Weather constraints on global drone flyability. Scientific Reports, 11(1): 12092. https://doi.org/10.1038/s41598-021-91325-w

[13] Paz, C., Suárez, E., Gil, C., Baker, C. (2020). CFD analysis of the aerodynamic effects on the stability of the flight of a quadcopter UAV in the proximity of walls and ground. Journal of Wind Engineering and Industrial Aerodynamics, 206: 104378. https://doi.org/10.1016/j.jweia.2020.104378

[14] Paterson, D.A., Apelt, C.J. (1990). Simulation of flow past a cube in a turbulent boundary layer. Journal of Wind Engineering and Industrial Aerodynamics, 35: 149-176. https://doi.org/10.1016/0167-6105(90)90214-W

[15] Yousif, M.Z., Lim, H. (2021). Improved delayed detached-eddy simulation and proper orthogonal decomposition analysis of turbulent wake behind a wall-mounted square cylinder. AIP Advances, 11(4): 045011. https://doi.org/10.1063/5.0045921

[16] Chang, C.H., Meroney, R.N. (2001). Numerical and physical modeling of bluff body flow and dispersion in urban street canyons. Journal of Wind Engineering and Industrial Aerodynamics, 89(14-15): 1325-1334. https://doi.org/10.1016/S0167-6105(01)00129-5

[17] Zedan, A.S.A., Ayad, S.S., Abdel-Hadi, E.A., Gaheen, O.A.M. (2006). Large eddy simulation for flow around buildings. In Proceedings of ICFDP 8: Eighth International Congress of Fluid Dynamics & Propulsion, Sharm El-Shiekh, Sinai, Egypt.

[18] Saeedi, M., LePoudre, P.P., Wang, B.C. (2014). Direct numerical simulation of turbulent wake behind a surface-mounted square cylinder. Journal of Fluids and Structures, 51: 20-39. https://doi.org/10.1016/j.jfluidstructs.2014.06.021

[19] Bourgeois, J.A., Sattari, P., Martinuzzi, R.J. (2011). Alternating half-loop shedding in the turbulent wake of a finite surface-mounted square cylinder with a thin boundary layer. Physics of Fluids, 23(9): 095101. https://doi.org/10.1063/1.3623463

[20] Sattari, P., Bourgeois, J.A., Martinuzzi, R.J. (2012). On the vortex dynamics in the wake of a finite surface-mounted square cylinder. Experiments in Fluids, 52: 1149-1167. https://doi.org/10.1007/s00348-011-1244-6

[21] Cotteleer, L., Longo, R., Parente, A. (2022). Flow-based stress-blended eddy simulation (Fb-SBES): A new hybrid framework for urban flow CFD simulations. In International Conference on Building Energy and Environment, pp.149-157. https://doi.org/10.1007/978-981-19-9822-5_17

[22] Longo, R., Ferrarotti, M., Sánchez, C.G., Derudi, M., Parente, A. (2017). Advanced turbulence models and boundary conditions for flows around different configurations of ground-mounted buildings. Journal of Wind Engineering and Industrial Aerodynamics, 167: 160-182. https://doi.org/10.1016/j.jweia.2017.04.015

[23] Kotsiopoulou, M., Bouris, D. (2022). Numerical simulation of the effect of a single gust on the flow past a square cylinder. Fluids, 7(9): 303. https://doi.org/10.3390/fluids7090303

[24] Speziale, C.G. (1998). Turbulence modeling for time-dependent RANS and VLES: A review. AIAA Journal, 36(2): 173-184. https://doi.org/10.2514/2.7499

[25] Saeedi, M., Wang, B.C. (2016). Large-eddy simulation of turbulent flow around a finite-height wall-mounted square cylinder within a thin boundary layer. Flow, Turbulence and Combustion, 97: 513-538. https://doi.org/10.1007/s10494-015-9700-7

[26] OpenFOAM and The OpenFOAM Foundation. https://openfoam.org/.

[27] Menter, F.R. (1994). Two-equation eddy-viscosity turbulence models for engineering applications. AIAA Journal, 32(8): 1598-1605. https://doi.org/10.2514/3.12149

[28] Spalart, P.R. (1997). Comments on the feasibility of LES for wings and on the hybrid RANS/LES approach. In Proceedings of the First AFOSR International Conference on DNS/LES, Ruston, LA, pp. 137-147.

[29] Bouris, D., Bergeles, G. (1999). 2D LES of vortex shedding from a square cylinder. Journal of Wind Engineering and Industrial Aerodynamics, 80(1-2): 31-46. https://doi.org/10.1016/S0167-6105(98)00200-1

[30] Giersch, S., El Guernaoui, O., Raasch, S., Sauer, M., Palomar, M. (2022). Atmospheric flow simulation strategies to assess turbulent wind conditions for safe drone operations in urban environments. Journal of Wind Engineering and Industrial Aerodynamics, 229: 105136. https://doi.org/10.1016/j.jweia.2022.105136

NOMENCLATURE

d	Squared cylinder width
h	Squared cylinder height
U_∞	Free-stream wind mean velocity
u_i	Velocity component
x_i	Instant position
p	Pressure
$\bar{x}$	Any averaged quantity

Greek symbols

ρ	Air density
τ	Shear stress
μ	dynamic viscosity
ν	kinematic viscosity